Available online at www.sciencedirect.com
SCIENCE DIRECT®
Vibrational Spectroscopy 36 (2004) 47–55
VIBRATIONAL SPECTROSCOPY
www.elsevier.com/locate/vibspec

Raman, IR, and surface-enhanced Raman spectroscopy of papaverine An automated setup for in situ synthesis of the silver substrate and recording of the SER spectra

N. Leopold[a], J.R. Baena[b], M. Bolboacă[c], O. Cozar[a], W. Kiefer[c], B. Lendl[b,*]

[a]*Faculty of Physics, Babeş-Bolyai University, Kogălniceanu 1, 400084 Cluj-Napoca, Romania*
[b]*Institute of Chemical Technology and Analytics, TU Vienna, Getreidemarkt 9-164/AC, 1060 Vienna, Austria*
[c]*Institut für Physikalische Chemie, Universität Würzburg, Am Hubland, 97074 Würzburg, Germany*

Received 19 November 2003; received in revised form 25 February 2004; accepted 25 February 2004
Available online 19 May 2004

Abstract

Raman, IR, and surface-enhanced Raman scattering (SERS) were employed for the vibrational characterization of papaverine in the free and adsorbed state. The vibrational assignments were performed by means of density functional theory (DFT) calculations. The adsorption of the molecule was concluded with the isoquinoline and the benzene ring close to the silver surface in tilted orientations. Employing a sequential injection system, an automatized setup was developed for reliable, accurate and rapid recording of FT-SER spectra. The colloidal silver substrate was synthesized in situ in a 2 ml quartz cuvette by reducing silver nitrate with hydroxylamine. The FT-SER spectrum of papaverine obtained with the developed experimental setup exhibits the same characteristics as the SER spectrum obtained with a citrate reduced silver colloid.

Keywords: DFT; On-line monitoring; Papaverine; SERS

1. Introduction

Papaverine (Fig. 1) is an alkaloid found in opium and therefore produces a major interest in forensic sciences. Several studies concerning the employment of spectroscopic methods for the detection of papaverine as a marker for heroin were performed in the last years, [1–4] and methods for rapid detection of papaverine at low concentrations are under continuous improvement [5,6]. Papaverine is also a pharmacological compound being used as muscle relaxant and vasodilator. Therefore, the physiological properties of the molecule and the interaction of papaverine with other biomolecules were extensively studied [7–9].

Raman scattering provides useful structural information making it a powerful molecular investigation tool. With the development of diode lasers and sensitive detectors in the last decade, Raman is becoming an increasingly popular technique for biomedical applications such as the identification or characterization of biological materials. [10] Raman spectroscopy has been successfully applied in the study of various drugs, including pharmaceuticals, [11] narcotics [12], and drug delivery devices, [13,14] the Raman methods offering a range of significant advantages over other spectroscopic techniques, including no requirements of sample preparation, in situ analysis, investigation of aqueous solutions, rapid identification, analysis of drug mixtures, identification of contaminants in samples, characterization of formulated materials, and process monitoring.

Disadvantages of normal Raman spectroscopy for applications within the pharmaceutical industry are due to the problems associated with fluorescence and the weak Raman scattering process, which leads to the need for intense laser excitation sources and sensitive detectors.

A suitable alternative with versatile opportunities to overcome the frequent inconveniences of fluorescence and low sensitivity of Raman spectroscopy is offered by surface-enhanced Raman (SER) spectroscopy. When the molecules are adsorbed on rough metal surfaces, the Raman cross-section is enhanced by several orders of magnitude, in some cases even up to 14th order, and fluorescence may be quenched [15–19]. The potential to combine high sensitivity with the structural information content of Raman spectroscopy makes SER spectroscopy a powerful tool in a variety of fields, [20,21] including biospectroscopy [22]. However,

* Corresponding author. Tel.: +43-1-5880115140; fax: +43-1-5880115199.
E-mail address: blendl@mail.zserv.tuwien.ac.at (B. Lendl).

0924-2031/$ – see front matter © 2004 Elsevier B.V. All rights reserved.
doi:10.1016/j.vibspec.2004.02.008

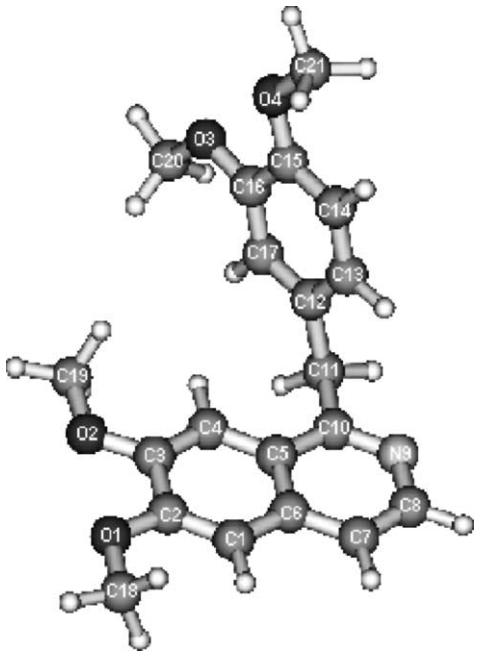

Fig. 1. Chemical structure of papaverine. Optimized geometry calculated at the BPW91/6-31+G* level of theory.

the use of surface-enhanced Raman scattering (SERS) as analytical technique presents important practical problems, the main drawback being the production of reproducible SERS substrates. A well-known problem is the degradation of SERS surfaces upon multiple use, together with the appearance of memory effects, that preclude the repetitive use of the same substrate; in addition, conventional approaches to synthesize active SERS colloids do not present good batch to batch reproducibility (typical R.S.D. values around 30%). To solve these problems, flow systems have been employed to improve the reproducibility of the results, either for the synthesis of batches of stabilized colloids [23] or for the on-line generation and use of the substrates [24,25].

The implementation of swift and safe drug development processes is, clearly, a priority for the pharmaceutical industry. Many techniques including IR spectroscopy, NMR, XRD, high-performance liquid chromatography, and thermal methods have been developed in order to offer automated analyses, though automatized Raman analyses at industrial level are less represented as other spectroscopic methods. Nevertheless, latest developments concerning on-line measurements employing SER spectroscopy are promissory. [23–26] In this work, Raman and SER spectra of papaverine were recorded and the assignments of papaverine vibrational modes were accomplished on the basis of density functional theory (DFT) calculations. To the best of our knowledge, a SERS investigation or a complete vibrational analysis of papaverine is missing in the literature. In order to combine the structural information and sensitivity provided by SERS with the accuracy of flow injection analysis (FIA), an automatized experimental setup was developed for in situ synthesis of the colloidal silver substrate and recording of accurate and reliable SER spectra. In a previous paper [25], we reported a similar setup where the sample is miniaturized, the SERS substrate preparation, and analyte addition occurring in an acoustically levitated nanoliter droplet. The experimental setup described here desires to verify the applicability of the developed setup in the milliliter range by using a common quartz cuvette and when using papaverine as analyte.

2. Experimental

2.1. Chemicals

All the employed chemicals were reagent grade or better. Stock solutions of silver nitrate (Merck, Darmstadt, Germany), hydroxylamine hydrochloride (Fluka, Vienna, Austria), sodium hydroxide (Sigma–Aldrich, Vienna, Austria), trisodium citrate (Sigma–Aldrich), sodium chloride (Sigma–Aldrich), crystal violet (Sigma–Aldrich), and papaverine hydrochloride (Sigma–Aldrich) were prepared by dissolving the proper amounts of the reagents in distilled water.

2.2. Apparatus

The FT-SER spectra were recorded with a Bruker FRA 106 Raman accessory attached to a Bruker IFS 66 FT-IR spectrometer equipped with a liquid nitrogen cooled Ge detector. The 1064 nm Nd:Yag laser was used as excitation source and the laser power was set to 200 mW. The FT-SER spectra were recorded in backscattering geometry with a resolution of 8 cm^{-1}.

Raman and SER spectra of papaverine were also recorded employing a Dilor LabRam spectrometer with 1800 grooves per mm diffractive grating. The 514.5 nm output of a Spectra Physics argon ion laser was used as excitation line and the laser power was kept below around 100 mW. The Raman and SER spectra were collected in backscattering geometry and the spectral resolution was 4 cm^{-1}. The detection system consisted of a Peltier cooled charge-coupled device detector.

The FT-IR spectrum was obtained with a Bruker IFS 25 spectrometer with a resolution of 2 cm^{-1}. Pellets for IR measurements were prepared by dispersing papaverine hydrochloride in potassium bromide.

2.3. Experimental setup for on-line SER measurements

Fig. 2 shows the experimental setup used for in situ preparation of SERS substrate in a 2 ml quartz cuvette and on-line monitoring by FT-Raman spectroscopy.

The sequential injection (SI) system was built with a Cavro XP 3000 syringe pump (Sunnyvale, CA, USA) equipped with a 1 ml syringe. A Valco 6 port selection valve

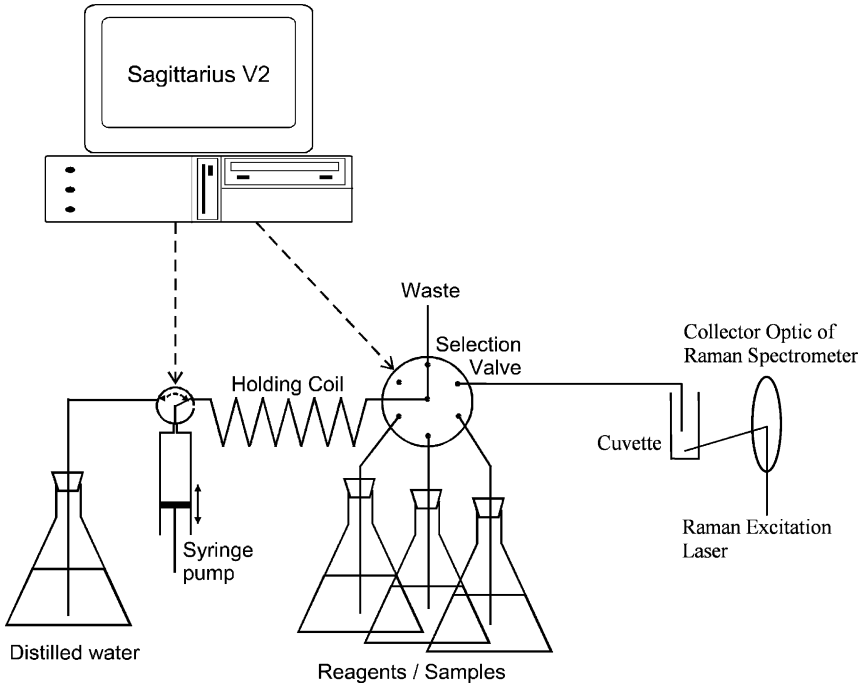

Fig. 2. Experimental setup comprising an automated flow system enabling sequential introduction of the reagents and analytes into the cuvette placed in the sample compartment of a FT-Raman spectrometer.

(Houston, TX, USA) was also employed. PTFE tubings (Global FIA, Gig Harbor, WA) with inner diameters of 0.25 and 0.75 mm were used for the flow system. The pump and the valve of the SI system were controlled via the in-house written MS Visual Basic 6.0 based software Sagittarius V2 (1.2.0003). From the selection valve a tubing with an 0.25 mm inner diameter made the connection with the 2 ml quartz cuvette, placed in the sample compartment of the FT-Raman spectrometer. The computer-controlled flow system enabled sequential introduction of the reagents and analytes into the cuvette.

2.4. Calculations

DFT calculations of the structure and vibrational wave numbers of the free papaverine molecule as well as Ag–papaverine complex were performed using the Gaussian 98 program package. [27] The theoretical calculations were carried out with Becke's 1988 exchange functional [28] and the Perdew–Wang 91 gradient corrected correlation functional [29] (abbreviated as BPW91). The Los Alamos effective core potential plus double zeta [30–32] (LanL2DZ) was employed for the silver atom, whereas the 6-31+G* Pople split-valence polarization basis set was used in the geometry optimization and normal modes calculations for the other atoms. At the optimized structure of the examined species no imaginary frequency modes were obtained, proving that a local minimum on the potential energy surface was found. The optimized geometry of the papaverine molecule calculated at the BPW91/6-31+G* level of theory is presented in Fig. 1.

3. Results and discussion

Vibrational characterization of papaverine. Fig. 3 presents the Raman and FT-IR spectra of papaverine hydrochloride in solid state. The Raman spectrum is the result of one accumulation of 100 s exposure time employing the 514.5 nm laser line.

The assignment of the bands appearing in the FT-IR and Raman spectra was accomplished by using high DFT quantum chemical calculations. Table 1 contains the main wave numbers of the experimentally obtained IR and Raman spectra of solid papaverine and the calculated wave numbers (unscaled values) of the papaverine molecule.

Papaverine is available as papaverine hydrochloride, therefore sodium hydroxide solution was added to increase the pH of the papaverine solution. The highest obtained pH value was 6.5, a further addition of the sodium hydroxide leading to the desolvation of papaverine from the solution. This fact is supposed to be due to the deprotonation process of the papaverine molecules at this pH, whereas the unprotonated molecular species are weakly soluble in water. Therefore, both molecular species, the protonated and the unprotonated, contribute to the Raman spectrum of papaverine (10^{-2} M) in aqueous solution at pH 6.5. This can be observed in Fig. 4a by the presence of bands at 1411 and 1364 cm^{-1} which are characteristic for the protonated and unprotonated forms of the analyte [33].

The Raman spectrum is the result of two accumulations of 200 s exposure time employing the 514.5 nm laser line. The assignments of the bands of the Raman spectrum of papaverine in aqueous solution can be found in Table 1.

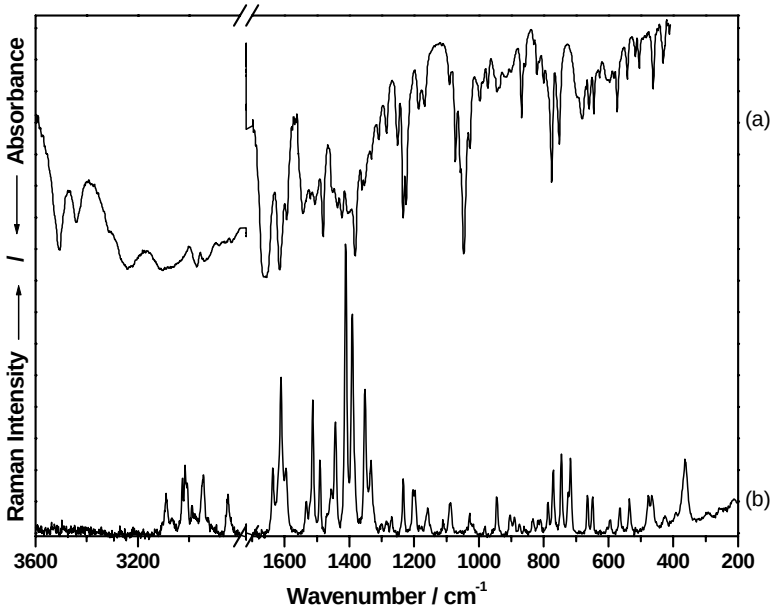

Fig. 3. (a) FT-IR and (b) Raman spectra of solid papaverine hydrochloride.

A strict comparison between the experimental and calculated wave numbers and intensities (Table 1) is not possible, because the experimental data were obtained for papaverine in solid state and aqueous solution, whereas the theoretical results correspond to papaverine in the gas phase. The calculated wave numbers are obtained using the harmonic approximation for the interatomic interactions in the molecule, whereas the experimental wave numbers are anharmonic by nature. Moreover, the Raman and IR spectra of papaverine in solid state are due to the protonated molecular form of papaverine and also, the protonated molecular species contribute to the Raman spectrum of papaverine in aqueous solution. Nevertheless, as can be observed from Table 1 the quality of the quantum chemical results at the presented theoretical levels are sufficient to be useful for the assignment of the experimental data.

For obtaining of the SER spectra a citrate reduced silver colloid, prepared according to the Lee–Meisel procedure [34] was used. The pH of the silver colloid was 6.5, the same as when recording the Raman spectrum of papaverine in aqueous solution. Firstly, 10 μl of 10^{-2} M papaverine solution from the amount used for the Raman spectrum (Fig. 4a) were added to 1 ml silver colloid with a microliter syringe. Secondly, 50 μl of 10^{-3} M NaCl solution were added to the cuvette for a better aggregation of the silver colloidal particles, leading to a better Raman enhancement. The final concentration of papaverine in the silver colloidal solution was 9.4×10^{-5} M. Fig. 4b presents the recorded SER spectrum of papaverine, which is the result of one accumulation of 150 s exposure time using the 514.5 nm laser line.

By comparing the Raman spectrum (Fig. 4a) to the SER spectrum (Fig. 4b) one can see that most of the peaks are shifted to lower wave numbers evidencing a chemisorption of the papaverine molecule to the silver surface. Most of the bands from the Raman spectrum can be retrieved in the SER spectrum. According to the electromagnetic field enhancement theory of SERS, the field enhancement rapidly decreases with increasing distance from the metal surface [20]. Vibrations belonging to the isoquinoline ring at 1394 and 1423 cm^{-1} (Table 1) and benzene ring at 362 and 1355 cm^{-1} (Table 1) are present in the SER spectrum (Fig. 4b). Consequently, it can be concluded that both rings lay in the vicinity of the silver surface. Most probably, the papaverine molecule adsorbs through the lone pair electrons of the nitrogen atom from the isoquinoline ring, so that the isoquinoline and the benzene ring are tilted oriented to the silver surface. The Ag–N vibration is evidenced by the strong band at 232 cm^{-1}. Table 1 also contains the main wave numbers of the SER spectrum and the calculated wave numbers (unscaled values) of the papaverine molecule when a silver atom is attached to the nitrogen atom from the isoquinoline ring. Also in this case, a strict comparison between the theoretical wave numbers and experimental ones is not possible because a simple attachment of an Ag atom can not reproduce the complexity of the SERS effect. However, the calculations performed on this papaverine–Ag model SERS complex could be regarded as a first step that contributes to a better understanding of the chemisorption effect on the vibrational behavior of the adsorbed molecule.

On-line FT-SER measurements. Employing the setup described in Section 2 (Fig. 2), starting from the reagents silver nitrate solution and hydroxylamine hydrochloride in basic solution and the analyte solution, after a time range of 150 s the FT-SER spectrum of the analyte was obtained. The preparation and characterization of the hydroxylamine reduced silver colloids was comprehensively described elsewhere [25,35].

Table 1
The experimental IR, Raman, SER and the calculated wave numbers (cm^{-1}) of the free papaverine molecule and the Ag–papaverine complex

IR	Raman solid	Raman liquid	SERS	Calculation[a]	Calculation[b]	Assignment
	152 m			151	156	C2O1, C3O2, C16O3, C15O4 twist
	190 w			198	197	CH3 + CH2 def
	211 w		232 s	207	212	CH3 + CH2 def
					242	CH3 + CH2 def + Ag–N str
	249 w			244	245	CH3 + CH2 def
	294 w			296	298	Ring 1 out of plane def + CH3 (C18, C19) def
	361 m	371 s	362 s	360	357	Ring 2 out of plane def + CH2 def
411 w	390 w			406	411	CH2 def
424 sh				449	453	C1C2O1, C4C3O2 wag
430 m	422 w			452	457	C1C2O1, C4C3O2 wag
461 m	465 m	466 w	466 w	459	461	C17C16O3, C14C15O4 wag
	475 m	485 w	485 w	476	478	C1C6C7, C4C5C10 wag
516 m		536 w	528 w	519	519	Ring 1 + ring 2 out of plane def
540 m	534 m			554	552	Ring 1 + ring 2 out of plane def
573 m	564 m	563 w	573 w	566	563	Ring 1 + ring 2 out of plane def
595 m	592 w			598	595	Ring 1 + ring 2 out of plane def
604 m	602 w			617	619	C1C2O1, C4C3O2 bend
626 m	627 w			632	639	Ring1 + ring2 in plane def
644 m	647 m	654 w	647 w	649	653	Ring 1 + ring 2 in plane def
659 m				678	689	C1C2O1, C4C3O2, C17C16O3, C14C15O4 twist
668 sh	663 m	671 w	661 w	688	694	C1C2O1, C4C3O2, C17C16O3, C14C15O4 twist
	716 m	722 m	714 m	721	715	Ring 1 + ring 2 out of plane def+ C10C11C12 def
	722 sh	735 m	725 m	725	727	Ring 1 + ring 2 out of plane def+ C10C11C12 def
752 s	744 m	739 m	737 sh	761	761	Ring 1 in plane def
776 s	770 m	776 m	765 m	769	766	CH wag
	784 m	794 w	781 w	787	782	CH wag
800 m	809 w			790	790	CH twist
813 sh	815 w			814	819	CH twist
831 sh	831 w			830	836	CH twist
868 m	873 w			876	866	Ring 1 in plane def
	889 w			884	882	CH twist (ring2) + CH2 def
901 m	902 m	900 w	892 w	906	912	CH twist (ring2) + CH2 def
917 m	923 w	923 w	916 w	925	921	CH twist (ring2) + CH2 def
943 m	944 m	953w	947 w	939	947	C10C11C12 def + CH2 def
987 sh	980 w			992	994	C10C11C12 def + CH2 def
1027 m	1028 m	1031 w	1034 w	1034	1033	Trigonal str (ring1, ring2)
1047 s	1044 w			1041	1040	Trigonal str (ring1, ring2)
1073 s	1078 sh			1052	1052	C18O1, C19O2, C20O3, C21O4 str
	1086 m	1086 m	1082 m	1082	1086	C18O1, C19O2, C20O3, C21O4 str
1091 m	1109 w			1111	1116	CH bend (ring2)
	1147 sh			1146	1145	CH bend (ring2)
1168 m	1156 m	1155 w	1168 w	1161	1160	C11C12 str + CH bend (ring2)
	1195 m	1201 sh	1188 w	1199	1200	C2O1, C3O2 str + CH rock (ring 1)
	1201 m	1209 w	1207 w	1216	1218	CH bend (ring 1) + C10C11 str
1225 s	1224 sh			1237	1238	CH bend (ring 2) + C15O4, C16O3 str
1234 s	1232 m	1242 w	1233 w	1242	1246	CH rock (ring 1, ring 2) + CH2 def
1251 s	1267 w	1270 w	1271 w	1266	1269	CH rock (ring1, ring2) + CH2 def
1284 m	1284 w			1282	1282	CH rock (ring 1, ring 2) + C2O1, C3O2, C16O3, C15O4 str
1308 m	1299 w			1302	1306	CH rock (ring 1, ring 2) + CH2 def
1330 m	1331 m			1323	1325	CH2 def + CC str (ring 1, ring 2)
1352 m	1349 m			1353	1358	Ring 2 str
1361 m		1364 s	1355 s	1370	1376	Ring 2 str
1381 s	1388 s			1379	1386	Ring 2 str
1403 s	1409 s	1411 s	1394 s	1391	1394	Ring 1 str
1423 s	1423 sh	1423 s	1423 s	1424	1421	Ring 1 str
1436 m	1441m	1446 m	1448 w	1443	1443	CH3, CH2 def
1451 m	1451 sh			1452	1449	CH3, CH2 def
	1463 sh	1463 w	1463 w	1462	1464	CH3, CH2 def
1480 s	1487 m	1489 w	1482 m	1487	1484	CH3, CH2 def
1506 m	1509 m	1498 m	1509 m	1516	1518	Ring 1 + ring 2 str
1520 m	1528 m	1518 m	1518 sh	1523	1523	Ring 1 + ring 2 str
1544 m		1558 w	1543 w	1564	1562	Ring 1 + ring 2 str

Table 1 (*Continued*)

IR	Raman solid	Raman liquid	SERS	Calculation[a]	Calculation[b]	Assignment
1592 m	1592 m	1576 w	1564 w	1589	1591	Ring 1 + ring 2 str
	1606 m	1600 sh	1591 sh	1593	1595	Ring 1 + ring 2 str
1614 s	1615 sh	1619 sh	1604 m	1612	1612	Ring 1 + ring 2 str
1645 s	1632 m			1623	1622	Ring 1 + ring 2 str
2835 m	2843 m	2855 m	2841 m	2877	2878	CH str (CH2, CH3)
2857 m				2898	2900	CH str (CH2, CH3)
2881 m	2894 w		2917 sh	2904	2907	CH str (CH2, CH3)
2928 sh	2921 sh	2959 m	2940 m	2946	2946	CH str (CH2, CH3)
2941 m	2941 m			2971	2974	CH str (CH2, CH3)
2969 w	2973 w			3001	3008	CH str (CH2, CH3)
	3012 m		3020 m	3058	3054	CH str (ring 1, ring 2)
	3022 m		3077 m	3065	3063	CH str (ring 1, ring 2)
	3065 m			3089	3090	CH str (ring 1, ring 2)
3088 sh	3086 m			3110	3111	CH str (ring 1, ring 2)

[a] Calculations for the free molecule at the BPW91/6-31+G* level of theory.

[b] Calculations for the Ag–papaverine complex at the BPW91/Gen 5d Pseudo: LanL2, N, C, O, H 6-31+G*, Ag LanL2DZ level of theory, w: weak, m: medium, s: strong, sh: shoulder, ring 1: isoquinoline ring, ring 2: benzene ring, def: deformation, str: stretching, bend: bending, rock: rocking, wag: waging, and twist: twisting.

For the optimization of the setup and the in situ silver colloid preparation, crystal violet was employed as analyte due to its strong SER signal. Firstly, 800 μl silver nitrate (1.1×10^{-3} M) was pumped in the cuvette. Secondly, 90 μl of hydroxylamine hydrochloride–sodium hydroxide mixture (1.5×10^{-2} M/3×10^{-2} M) were added, the last stream also performing the mixing of the two reagents, silver nitrate and hydroxylamine solutions in the cuvette. Therefore, a flow rate for the hydroxylamine solution of 0.5 ml/s was found to be optimal so that in a few seconds a SERS active silver colloid with an extinction maximum at about 416 nm was obtained. After the addition of each reagent, 50 μl of water were flushed through the tubing connecting the selection valve and the cuvette, in order to clean it from residues of the previous reagents. Thirdly, 25 μl sodium chloride (4×10^{-1} M) were added for a better Raman enhancement. Finally, 100 μl crystal violet (10^{-5} M) as analyte were pumped into the cuvette. The final concentration of crystal violet in the silver sol was 8.9×10^{-7} M.

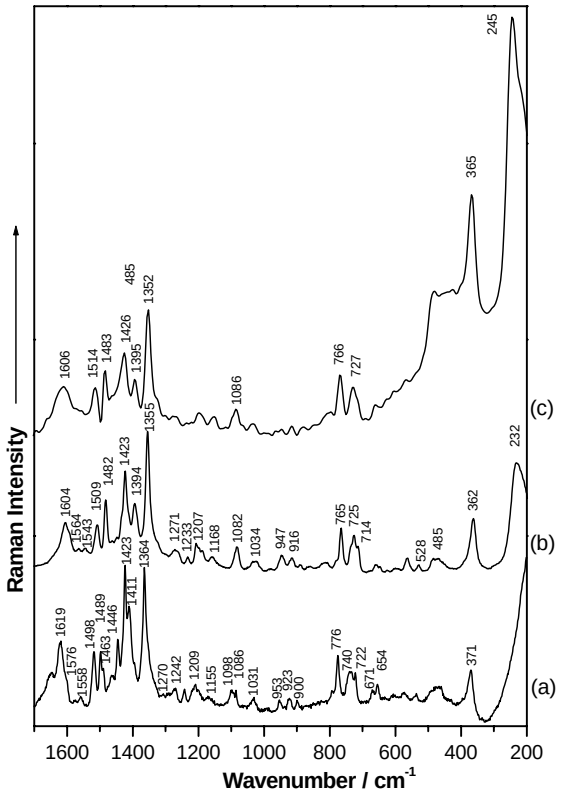

Fig. 4. (a) Raman spectrum of aqueous solution of papaverine. (b) SER spectrum of papaverine using a citrate reduced silver colloid and employing the 514.5 nm laser line. (c) FT-SER spectrum of papaverine obtained with the automated setup.

Fig. 5 presents the time evolution of the synthesis of the silver substrate and the recorded FT-SER spectra of crystal violet. The experiment is recorded from the initial mixing of silver nitrate and hydroxylamine hydrochloride, followed by the addition of the analyte.

Each spectrum is the result of eight accumulated scans. In the first 140 s, during the silver colloid synthesis, no bands are seen in the spectra as the concentration of the reagents is too low for obtaining Raman spectra under these experimental conditions. The FT-SER spectra of crystal violet were obtained after 150 s from the beginning of the experiment. Generally, different degrees of aggregation and particle sizes in metal colloids have been identified as potential sources of differences in enhancement factors [36]. It can be seen in Fig. 5 that the intensity of the peaks increases in time. This fact is due to the aggregation process of the silver particles in time, determining a higher extinction of the silver aggregates at 1064 nm [20,25]. However, the experiment was repeated many times and the success rate was found to be greater than 90%.

Once the experimental setup was optimized, papaverine was employed as analyte. Fig. 6 presents the recorded FT-SER spectra of papaverine using the automatized setup.

The synthesis of the silver substrate was done in the same way as described above when crystal violet was used as

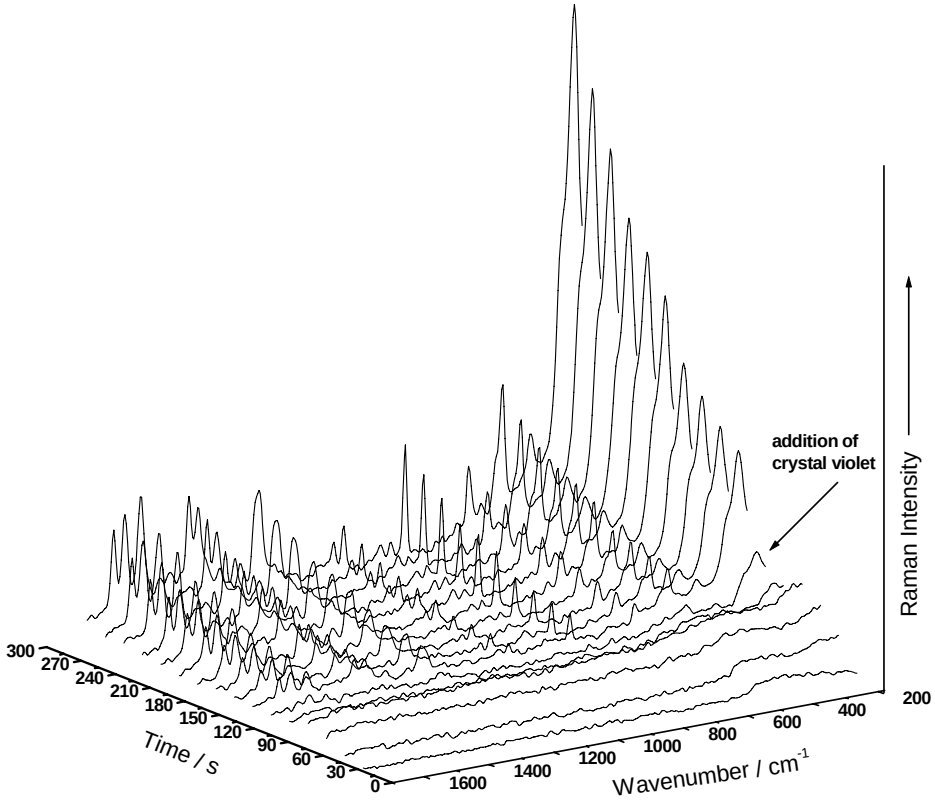

Fig. 5. Time evolution of the processes in the cuvette as monitored by FT-Raman spectroscopy, comprising silver sol synthesis followed by addition of the analyte crystal violet.

analyte. During the synthesis of the silver colloid a peak at 1121 cm^{-1} appears due to a momentaneous excess of nitrate in the solution that is then consumed and the peak is disappearing after ~60 s. [37] It has to be noted that the peak was not shown in the spectra from Fig. 5 because in that case the S/N ratio was considerable smaller and also the scan time was 4 times shorter than in the spectra shown in Fig. 6. Once the silver substrate was synthesized, 150 μl of papaverine solution (2.7×10^{-2} M) were pumped in the cuvette followed by 100 μl sodium chloride (4×10^{-1} M) for a better Raman enhancement. Experimentally, it was found that the addition of sodium chloride after papaverine a proper aggregation of the colloidal silver particles takes place, as when adding the sodium chloride solution before the analyte. The final concentration of papaverine in the silver sol was 3.3×10^{-3} M. The SER intensities for papaverine are lower than those of crystal violet, therefore the number of scans was increased to 32 for each spectrum.

For the SERS enhancement, the absorption coefficient of the complexes formed by the silver aggregates and the adsorbed molecules at the excitation laser wavelength is of great importance. Particularly, the lower SERS intensities of papaverine than those of crystal violet can be explained by a possible weaker absorption coefficient of the complexes papaverine–silver aggregates at 1064 nm than the absorption coefficient of the complexes crystal violet–silver aggregates at 1064 nm. As discussed above, when the 514.5 nm laser line was employed the concentration of papaverine in the SER spectra was more than 2 orders of magnitude lower (9.4×10^{-5} M).

The changes in the SERS intensities levels of in the first 32 s after the analyte is added. The final concentrations of crystal violet was 8.9×10^{-7} M while that for papaverine was much higher at 3.3×10^{-3} M. At these concentrations, coverage of the silver would be about a monolayer for the crystal violet and greater than one monolayer for the papaverine. Once a monolayer is formed, little or no additional increase in signal occurs because additional layers are not appreciably enhanced due to the strong gradient fall with distance of the electromagnetic field created by the silver particles.

As it can be seen from Fig. 6, the spectral ''fingerprint'' of papaverine with the main peaks at 365, 766, 1086, 1352, 1426, 1483, 1514, and 1606 cm^{-1} is clearly evident in the FT-SER spectra. The experiment was repeated and the success rate was found to be greater than 90%, the peaks position being each time the same.

To test the accuracy of the automated setup and the properties of the in situ synthesized hydroxylamine reduced silver colloid, the recorded FT-SER spectrum of papaverine was compared with the SER spectrum recorded employing the citrate reduced silver colloid presented in Fig. 4b and c presents the FT-SER spectrum of papaverine recorded employing the automated setup as described above, the concentration of papaverine in the silver colloid being

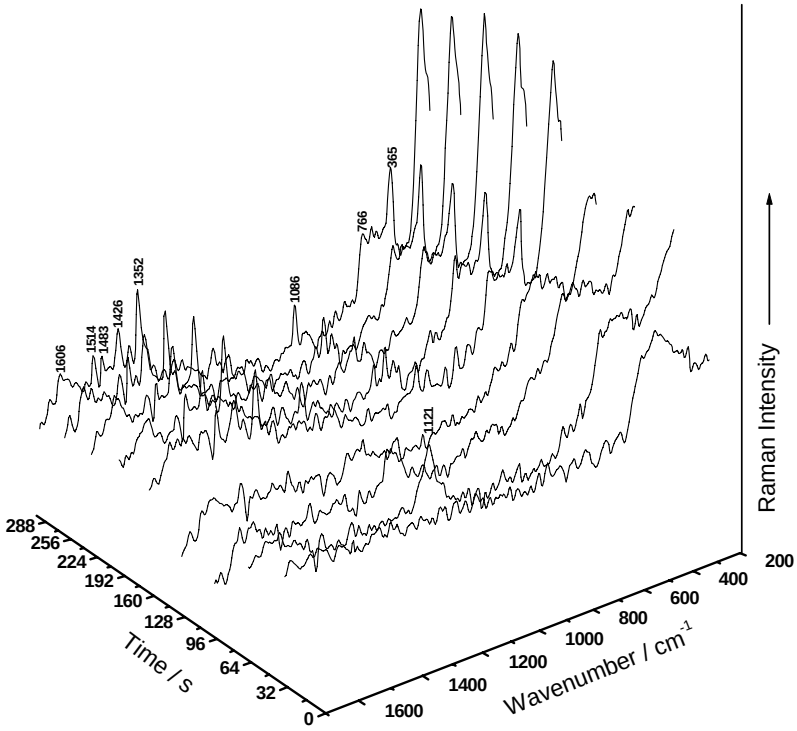

Fig. 6. Time evolution of the processes in the cuvette as monitored by FT-Raman spectroscopy, comprising silver sol synthesis followed by addition of the analyte papaverine.

3.3×10^{-3} M and the spectrum the result of 320 scans. The pH value of the silver colloid was 6.5, the same as when employing the citrate reduced colloid (Fig. 4b). Employing the 1064 nm laser line, the Raman enhancement is weaker than when employing the 514.5 nm laser line, due to a higher extinction of the silver aggregates at shorter wavelengths. Also, the SER spectrum from Fig. 4b shows narrower bands as it was recorded with a spectral resolution of 4 cm^{-1} while the SER spectrum from Fig. 4c was recorded with spectral resolution of 8 cm^{-1}.

Taking into account that the two SER spectra (Fig. 4b and c) were recorded with two different reduced silver substrates it is very probably that the orientation of papaverine to the two silver surfaces is not exactly the same, leading to several shifts in the bands. In Fig. 4c, the large band at about 400 cm^{-1} is due to a fluorescence band of the quartz cuvette.

Nevertheless, the most important conclusion that can be drawn is that the peak positions and relative intensities in the SER spectra of papaverine obtained with two different experimental setups and two different silver colloids exhibit the same characteristics.

4. Conclusions

The IR, Raman, and SER spectra of papaverine were recorded and assigned by means of DFT calculations. The SER spectrum show that the papaverine molecules are adsorbed with the isoquinoline and benzene rings close to the silver surface.

The high structure elucidating potential and sensitivity of SERS and the accuracy of automation were successfully combined for rapid recording of reliable FT-SER spectra. The FT-SER spectra obtained with the automated setup using the hydroxylamine reduced silver colloid and exciting with the 1064 nm laser line exhibit the same characteristics as the SER spectra recorded using a citrate reduced silver colloid and exciting with the 514.5 nm laser line. The development of standardized SERS substrates on a routine basis so that they become more reproducible and more easily prepared will expand analytical applications.

Acknowledgements

N.L. acknowledges M. Haberkorn for providing the Sagittarius software and useful discussions. M.B. and W.K. acknowledge financial support from the Deutsche Forschungsgemeinschaft and from the Fonds der Chemischen Industrie. J.R.B. also acknowledges a postdoctoral grant held by the Spanish Secretaría de Estado de Educación y Universidades and co-financed by the European Social Foundation.

References

[1] R. Brenneisen, F. Hasler, J. Forensic Sci. 47 (2002) 885.
[2] M.J. Bogusz, R.D. Maier, M. Erkens, U. Kohls, J. Anal. Toxicol. 25 (2001) 431.

[3] B.D. Paul, C. Dreka, E.S. Knight, M.L. Smith, Planta Med. 62 (1996) 544.
[4] V.C. Trenerry, R.J. Wells, J. Robertson, J. Chromatogr. A 718 (1995) 217.
[5] N.T. Abdel-Ghani, A.F. Shoukry, Y.M. Issa, O.A. Wahdan, J. Pharm. Biomed. Anal. 28 (2002) 373.
[6] M. Eisman, M. Gallego, M. Varcarcel, J. Pharm. Biomed. Anal. 12 (1994) 179.
[7] C.A. Ventura, G. Puglisia, M. Zappalab, G. Mazzonea, Int. J. Pharm. 160 (1998) 163.
[8] V.E. Yushmanov, J.R. Perussi, H. Imasato, M. Tabak, Biochim. Biophys. Acta 74 (1994) 1189.
[9] C.A. Ventura, M. Fresta, D. Paolino, S. Pedotti, A. Corsaro, G. Puglisi, J. Drug. Target 9 (2001) 379.
[10] L.A. Lyon, C.D. Keating, A.P. Fox, B.E. Baker, L. He, S.R. Nicewamer, S.P. Mulvaney, M.J. Natan, Anal. Chem. 70 (1988) 341R.
[11] L.S. Taylor, Am. Pharm. Rev. 4 (2001) 60.
[12] S.E.J. Bell, D.T. Burns, A.C. Dennis, J.S. Speers, Analyst 125 (2000) 541.
[13] A.C. Dennis, J.J. McGarvey, D.A. Woolfson, A. O'Grady, D.F. McCafferty, in: Proceedings of the XVIIth International Conference on Raman Spectroscopy, Beijing, 2000, pp. 1078.
[14] A.D. Woolfson, D.F. McCafferty, Int. J. Pharm. 94 (1993) 75.
[15] M. Moskovits, Rev. Modern Phys. 57 (1985) 783.
[16] A. Otto, J. Billmann, J. Eickmans, U. Ertuerk, C. Pettenkofer, Surf. Sci. 138 (1984) 319.
[17] A. Otto, I. Mrozek, H. Grabhorn, W. Akemann, J. Phys. Codens. Matter 76 (1992) 2444.
[18] J.A. Creighton, in: R.J.H. Clarck, R.E. Hester (Eds.), Spectroscopy of Surfaces, vol. 16, Wiley, New York, 1988, p. 37.
[19] A. Campion, P. Kambhampati, Chem. Soc. Rev. 27 (1988) 241.
[20] K. Kneipp, H. Kneipp, I. Itzkan, R.R. Dasari, M.S. Feld, Chem. Rev. 99 (1999) 2957.
[21] S. Nie, S.R. Emeroy, Science 275 (1997) 1102.
[22] T.M. Cotton, in: R.J.H. Clarck, R.E. Hester (Eds.), Spectroscopy of Surfaces, Wiley, New York, 1988, p. 91.
[23] R. Keir, E. Igata, M. Arundell, W.E. Smith, D. Graham, C. McHugh, J.M. Cooper, Anal. Chem. 74 (2002) 1503.
[24] L.M. Cabalin, A. Ruperez, J.J. Laserna, Talanta 40 (1993) 1741.
[25] N. Leopold, M. Haberkorn, T. Laurell, J. Nielson, J.R. Baena, J. Frank, B. Lendl, Anal. Chem. 75 (2003) 2166.
[26] S. Santesson, J. Johansson, L.S. Taylor, I. Levander, S. Fox, M. Sepaniak, S. Nilsson, Anal. Chem. 75 (2003) 2177.
[27] M.J. Frisch, G.W. Trucks, H.B. Schlegel, G.E. Scuseria, M.A. Robb, J.R. Cheeseman, V.G. Zakrzewski, J.A. Montgomery, Jr., R.E. Stratmann, J.C. Burant, S. Dapprich, J.M. Millam, A.D. Daniels, K.N. Kudin, M.C. Strain, O. Farkas, J. Tomasi, V. Barone, M. Cossi, R. Cammi, B. Mennucci, C. Pomelli, C. Adamo, S. Clifford, J. Ochterski, G.A. Petersson, P.Y. Ayala, Q. Cui, K. Morokuma, D.K. Malick, A.D. Rabuck, K. Raghavachari, J.B. Foresman, J. Cioslowski, J.V. Ortiz, A.G. Baboul, B.B. Stefanov, G. Liu, A. Liashenko, P. Piskorz, I. Komaromi, R. Gomperts, R.L. Martin, D.J. Fox, T. Keith, M.A. Al-Laham, C.Y. Peng, A. Nanayakkara, C. Gonzalez, M. Challacombe, P.M.W. Gill, B. Johnson, W. Chen, M.W. Wong, J.L. Andres, C. Gonzalez, M. Head-Gordon, E.S. Replogle, J.A. Pople, Gaussian 98, Revision A.7, Gaussian Inc., PA, Pittsburgh, 1998.
[28] A.D. Becke, Phys. Rev. A 38 (1988) 3098.
[29] J.P. Perdew, Y. Wang, Phys. Rev. B 45 (1992) 13244.
[30] P.J. Hay, W.R. Wadt, J. Chem. Phys. 82 (1985) 270.
[31] W.R. Wadt, P.J. Hay, J. Chem. Phys. 82 (1985) 284.
[32] P.J. Hay, W.R. Wadt, J. Chem. Phys. 82 (1985) 299.
[33] S. Cîntă-Pînzaru, N. Leopold, I. Pavel, W. Kiefer, ''Raman, SERS and theoretical studies of papaverine hydrochloride and its neutral species'', Spectrochim. Acta Part A: Mol. Biomol. Spectrosc., in press.
[34] P.C. Lee, D.J. Meisel, J. Phys. Chem. 86 (1982) 3391.
[35] N. Leopold, B. Lendl, J. Phys. Chem. B. 107 (2003) 5723.
[36] J.J. Laserna, Anal. Chim. Acta 283 (1993) 607.
[37] M.J. Ayora Cañada, A. Ruiz Medina, J. Frank, B. Lendl, Analyst 127 (2002) 136;
R. Keir, D. Sadler, W.E. Smith, Appl. Spectrosc. 56 (2002) 551–559.